Behavioral/Systems/Cognitive

Primitive Roles for Inhibitory Interneurons in Developing Frog Spinal Cord

W.-C. Li,[1] Shin-ichi Higashijima,[2] D. M. Parry,[1] Alan Roberts,[1] and S. R. Soffe[1]

[1]School of Biological Sciences, University of Bristol, Bristol BS8 1UG, United Kingdom, and [2]Department of Neurobiology and Behavior, State University of New York, Stony Brook, New York 11794-5230

Understanding the neuronal networks in the mammal spinal cord is hampered by the diversity of neurons and their connections. The simpler networks in developing lower vertebrates may offer insights into basic organization. To investigate the function of spinal inhibitory interneurons in *Xenopus* tadpoles, paired whole-cell recordings were used. We show directly that one class of interneuron, with distinctive anatomy, produces glycinergic, negative feedback inhibition that can limit firing in motoneurons and interneurons of the central pattern generator during swimming. These same neurons also produce inhibitory gating of sensory pathways during swimming. This discovery raises the possibility that some classes of interneuron, with distinct functions later in development, may differentiate from an earlier class in which these functions are shared. Preliminary evidence suggests that these inhibitory interneurons express the transcription factor engrailed, supporting a probable homology with interneurons in developing zebrafish that also express engrailed and have very similar anatomy and functions.

Key words: **locomotion; glycine; inhibition; spinal; interneuron; transcription**

Introduction

The definition of spinal interneuron classes according to their anatomy and physiological functions continues to be a very slow process. The problems of identifying spinal interneuron classes in mammals by their inputs (whether they are excitatory or inhibitory), their output target neurons, and their roles during responses have been emphasized recently (Jankowska, 2001). However, the differential expression of transcription factors is now beginning to unscramble the developmental origins of different classes of spinal interneurons in the mouse and the chick (Lee and Pfaff, 2001; Goulding et al., 2002; Helms and Johnson, 2003). This work on development points to common features shared by different classes of vertebrate and supports the view that the study of simpler groups can give us insights into the organization of more complex ones. Currently, the best understood spinal interneurons are probably those that coordinate locomotor movements in the adult lamprey and frog tadpole (Parker and Grillner, 2000; Roberts, 2000; Buchanan, 2001; Parker, 2003). Detailed information on spinal neuron classes is also becoming available for the developing zebrafish (Bernhardt et al., 1990; Hale et al., 2001). We can therefore look for parallels between spinal interneurons in these simpler vertebrate groups. Here, we examined the functions of a single, anatomically defined class of spinal inhibitory interneuron in the frog tadpole.

At the time of hatching from the egg, the *Xenopus* tadpole spinal cord may have as few as seven anatomical classes of neurons with different functions in reflex responses and swimming (Roberts, 2000; Li et al., 2001). These are shown diagrammatically in Figure 1, where their functions are listed. We have recently established that one class of spinal interneuron with a very characteristic axonal projection pattern, called ascending interneurons (aINs), produces phasic, glycinergic inhibition that gates sensory pathway interneurons during swimming. This inhibition allows reflex responses to touch to be coordinated with ongoing swimming (Sillar and Roberts, 1988; Li et al., 2002). Recordings show that spinal motoneurons and interneurons can also receive inhibition at the same phase in the swimming cycle as the inhibition of sensory pathway interneurons (Tunstall and Roberts, 1994). This raised the possibility that aINs have two inhibitory roles during locomotion: gating sensory transmission and controlling the firing of motoneurons and other central pattern generator (CPG) neurons.

Our aim was to use whole-cell patch recordings from pairs of spinal neurons in an immobilized preparation of the frog tadpole near the time of hatching to determine whether aINs have a second function providing inhibition to neurons that are components of the CPG for swimming. Spinal inhibitory interneurons with remarkably similar anatomy and physiology have been described in the zebrafish embryo (Higashijima et al., 2004). Because these zebrafish interneurons express the transcription factor engrailed, we sought evidence that aINs, as their possible homologs in *Xenopus*, were also positive for engrailed.

Received Dec. 3, 2003; accepted May 21, 2004.

This work was supported by the Wellcome Trust. We thank Drs. Rob Brownstone, Jon Clarke, John Isaac, Joe Fetcho, Robert Meech, and Daniel Robert for helpful comments on previous versions of this manuscript, Drs Y. Iwasaki and G. Thomsen for help with the *Xenopus* experiments at State University of New York, Dr. Alex Joyner for providing the *αEnhb-1* antiserum, and Derek Dunn, Jenny Maxwell, and Tim Colborn for technical help.

Correspondence should be addressed to Dr. Wen-Chang Li, School of Biological Sciences, University of Bristol, Woodland Road, Bristol BS8 1UG, UK. E-mail: wenchang.li@bristol.ac.uk.

DOI:10.1523/JNEUROSCI.1633-04.2004

 0270-6474/04/245840-●$15.00/0

Materials and Methods

Whole-cell patch recording. Details of the recording methods have been given recently (Li et al., 2002). Briefly, *Xenopus* tadpoles at stage 37/38 (Fig. 1) were anesthetized briefly with 0.1% MS-222 (3-aminobenzoic acid ester; Sigma, Poole, UK), immobilized in 10 μM α-bungarotoxin saline, then pinned in a bath of saline (in mM: 115 NaCl, 3 KCl, 2 $CaCl_2$, 2.4 $NaHCO_3$, 1 $MgCl_2$, and 10 HEPES, adjusted with 5 M NaOH to pH 7.4). In many paired recording experiments, 1 mM $MgCl_2$ was replaced by 1 mM $CaCl_2$. Skin and muscles over the right side of the spinal cord were removed, and a mid-dorsal cut was made along the spinal cord to open the neurocoel and expose neuronal cell bodies. Additional small cuts were made to expose more ventral neurons. The tadpole was then repinned in a small 700 μl recording chamber with a saline flow of ~2 ml per minute that allowed bright-field illumination from below on an upright Nikon E600FN microscope. Exposed neuronal cell bodies could be seen using a 40× water immersion lens. Antagonists were applied close to the recorded neuron soma using gentle pressure to solution in a pipette with tip diameter of 10–20 μm or dropped into a 100 μl well upstream to the recording chamber. The drugs used were bicuculline and strychnine (Sigma).

Extracellular recordings of ventral root activity were made using glass suction electrodes placed against the muscles. A stimulating suction electrode was placed on the tail skin to start fictive swimming activity. Patch pipettes were filled with 0.1% neurobiotin in intracellular solution (in mM: 100 K-gluconate, 2 $MgCl_2$, 10 EGTA, 10 HEPES, 3 Na_2ATP, and 0.5 NaGTP, adjusted to pH 7.3 with KOH) and had resistances ~10 M. In some experiments, 0.1% Alexa Fluor 488 (Molecular Probes, Eugene, OR) was also used in the patch pipette solution to identify neurons in live tadpoles. Junction potentials were corrected before making recordings. Signals were recorded with an Axoclamp 2B in conventional bridge or continuous single-electrode voltage-clamp mode, acquired with Signal software through a CED 1401 Plus interface with a sampling rate of 10 kHz. Off-line analyses were made with Minitab and Excel. All data were tested for normality (Anderson-Darling); median values are given for non-normal data; otherwise, all values are given as mean ± SD.

Processing for neuron anatomy. Once physiological testing was completed, the tadpoles were fixed in 2% glutaraldehyde in 0.1 M phosphate buffer (pH 7.2 at ~4°C). Dye-filling was successful through passive diffusion. After rinsing with 0.1 M PBS, the animals were: (1) washed in 1% Triton-X in PBS for 15 min twice; (2) incubated in a 1:300 dilution of extravidin peroxidase conjugate (Sigma) in PBS containing 0.5% Triton-X for 2–3 hr; (3) washed again in PBS; (4) presoaked in 0.08% DAB in PBS (DAB solution) for 5 min; (5) moved to 0.075% hydrogen peroxide in DAB solution for 5 min; and (6) washed in running tap water. The brain and spinal cord were then dissected free with the notochord and some ventral muscles, dehydrated, cleared in methyl benzoate and xylene, and mounted whole, between two coverslips, using Depex. Neurons were observed using a 100× oil immersion lens and traced using a drawing tube or photographed. To compensate for shrinkage during dehydration, all measurements in this study have been corrected by multiplying by 1.28 (Li et al., 2001).

En-1 staining. Tadpoles were fixed in 3.7% formaldehyde, 0.1 M 4-morpholinepropanesulfonic acid, 2 mM EGTA, and 1 mM $MgSO_4$ for 2 hr, rinsed in two changes of methanol, and stored overnight in methanol at −20°C. After rehydration, the spinal cord was exposed by dissection and the tissues were bleached in 15% hydrogen peroxide in PBS (120 mM NaCl in 0.1 M phosphate buffer, pH 7.2) for 2 hr. After a PBS wash, specimens were washed three times for 15 min in PBT (PBS with 0.1% Triton X100 and 20 mg/ml BSA) and then blocked in 10% normal goat serum in PBT (blocking buffer). They were then transferred to primary antiserum *αEnhb-1* (1:1000) (Davis et al., 1991) for 72 hr, washed five times for 1 hr in PBT, and incubated overnight in secondary antibody [peroxidase-conjugated $F(ab)_2$ fragment goat anti-rabbit IgG (Jackson Immunoresearch, West Grove, PA); diluted 1:500 in PBT]. After washing five times for 45 min in PBT, the peroxidase was visualized using nickel-enhanced DAB with glucose oxidase to generate the hydrogen peroxide. After two washes in PBS, specimens were cleared in Murrays Clear (2:1 benzyl benzoate:benzyl alcohol) and mounted between coverslips.

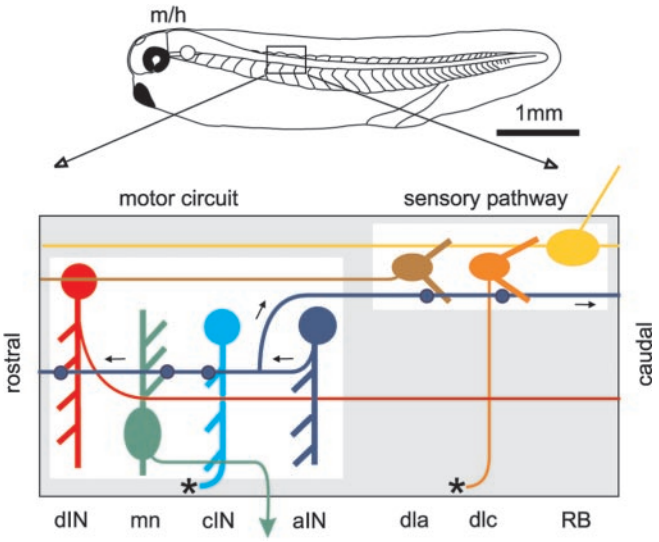

Figure 1. The tadpole and its spinal neurons. The *Xenopus* tadpole at the time of hatching (stage 37/38), with its head to the left, showing the eye, the border between midbrain and hindbrain (m/h), and the spinal cord lying under segmented swimming muscles. Below is a diagram of a length of spinal cord viewed from the side to show the neurons. Glycinergic aINs (purple) have ascending and descending axons that could contact and inhibit: dorsolateral commissural INs (dlc) and dorsolateral ascending INs (dla). These are excitatory sensory pathway interneurons, excited by skin sensory, touch-sensitive Rohon-Beard neurons (RB) that have no dendrites. aINs could also inhibit neurons that are active during swimming: mns, excitatory dINs, glycinergic reciprocal inhibitory cINs, and other aINs (data not shown). For each neuron class, the circle/oval is the soma; oblique lines indicate the dorsoventral extent of the dendrites; and the thin line shows the axon projection (asterisk indicates that the axon crosses ventrally to the opposite side). Each class of neuron actually forms a longitudinal column of 50–150 neurons on each side of the cord.

For stochastic expression of green fluorescent protein (GFP) in interneurons, a DNA construct having GFP under the control of the *Xenopus* neural β-tubulin promoter (kindly provided by Dr. B. Demeneix, Unité Mixte de Recherche-5166, Centre National de la Recherche Scientifique, Paris, France) was injected into one to four cell stage *Xenopus* embryos (5 pl of 20 ng/ml) (Coen et al., 2001). Embryos were fixed at stage 37/38. The spinal cords were dissected and processed with the anti-En1 antibody, as described by Higashijima et al. (2004). Retrograde labeling of spinal interneurons with rhodamine dextran was performed as described by Higashijima et al. (2004). After antibody staining, dissected spinal cords having GFP-labeled neurons were mounted in 70% glycerol. Samples having backfilled neurons were mounted in methyl salicilate after dehydration in series of methanol and clearing in a 1:2 mixture of benzyl benzoate and benzyl alcohol.

Cell type identification of *Xenopus* interneurons was more difficult than that of zebrafish interneurons because many neurons were labeled both by GFP labeling and backfilling. Only those examples in which we could follow the primary axon with confidence were included. Specimens were examined on a confocal microscope (LSM510; Zeiss, Thornwood, NY) (Higashijima et al., 2004).

Results

aINs inhibit spinal neurons active during swimming

To investigate whether aINs inhibited other CPG neurons, whole-cell patch recordings were made from 394 pairs of spinal neurons on the same side and in the rostral cord between segments 3 and 8 (between ~0.9 and 1.8 mm from the midbrain) (Fig. 2*B*, inset). In 51 cases, one of each pair was an aIN, and both neurons were rhythmically active during fictive swimming (Fig. 3*C*). Probable aINs were found during experiments by their characteristic pattern of firing during swimming that is delayed and

unreliable compared with motoneurons (Li et al., 2002). However, the identity of both neurons was confirmed anatomically after fixation and processing to show the neurobiotin injected from the patch electrode (Figs. 2*A*,*C*,*F*, 3*A*, 5*A*). In most cases, aINs had an ascending axon that formed a descending branch close to the soma. The dorsoventral position of somata and axons is difficult to judge after the dissection to allow whole-cell patch recording. In 10 of the 51 pairs, positive current sufficient to make the aIN fire led to short latency inhibition of the postsynaptic CPG neuron [5 commissural interneurons (cINs), 3 aINs, 1 motoneuron (mn), and 1 descending interneuron (dIN)] (Fig. 2*B*,*D*,*E*,*G*). In *Xenopus*, such short and consistent delays (1.0–3.6 msec with conduction distances of ~0.10–0.46 mm) indicate monosynaptic connections (Li et al., 2002, 2003). In all five cases tested, the inhibition was shown to be glycinergic because it was blocked by 2–5 μM strychnine (Fig. 3*B*).

The activity of the pairs of recorded neurons was also observed during fictive swimming, initiated by a 1 msec current pulse to the tail skin (Fig. 2*B*, inset). This excites the touch sensory nerve endings of Rohon-Beard neurons (Fig. 1), and the resulting swimming can be monitored by recording ventral root activity (Fig. 3*C*). Motoneuron and CPG neuron activity during swimming alternates on the left and right sides at frequencies of 10–20 Hz. Alternation is organized by glycinergic, reciprocal inhibition from cINs, seen as a "mid-cycle" IPSP (for review, see Roberts, 1990) (Fig. 3*C*). On each cycle, most CPG neurons fire a single impulse that is closely synchronized with the nearby ventral root burst. The firing of aINs during swimming is known to be less reliable and less well synchronized to the nearby ventral root burst than other CPG neurons (Li et al., 2002). In three cases, aIN spikes during swimming were followed at short latency by clear IPSPs in the other CPG neuron (Fig. 3*C*,*D*). Synchronizing the records to each presynaptic spike showed that the latency to these IPSPs was the same as the latency to IPSPs evoked by current injection into the aIN (Fig. 3*D*,*E*). The IPSPs, like the aIN spikes, were not synchronized and could occur anywhere in the early part of the swim cycle, before the start of the mid-cycle reciprocal inhibitory IPSP (Fig. 3*C*, asterisk). We therefore termed them "early-cycle" IPSPs.

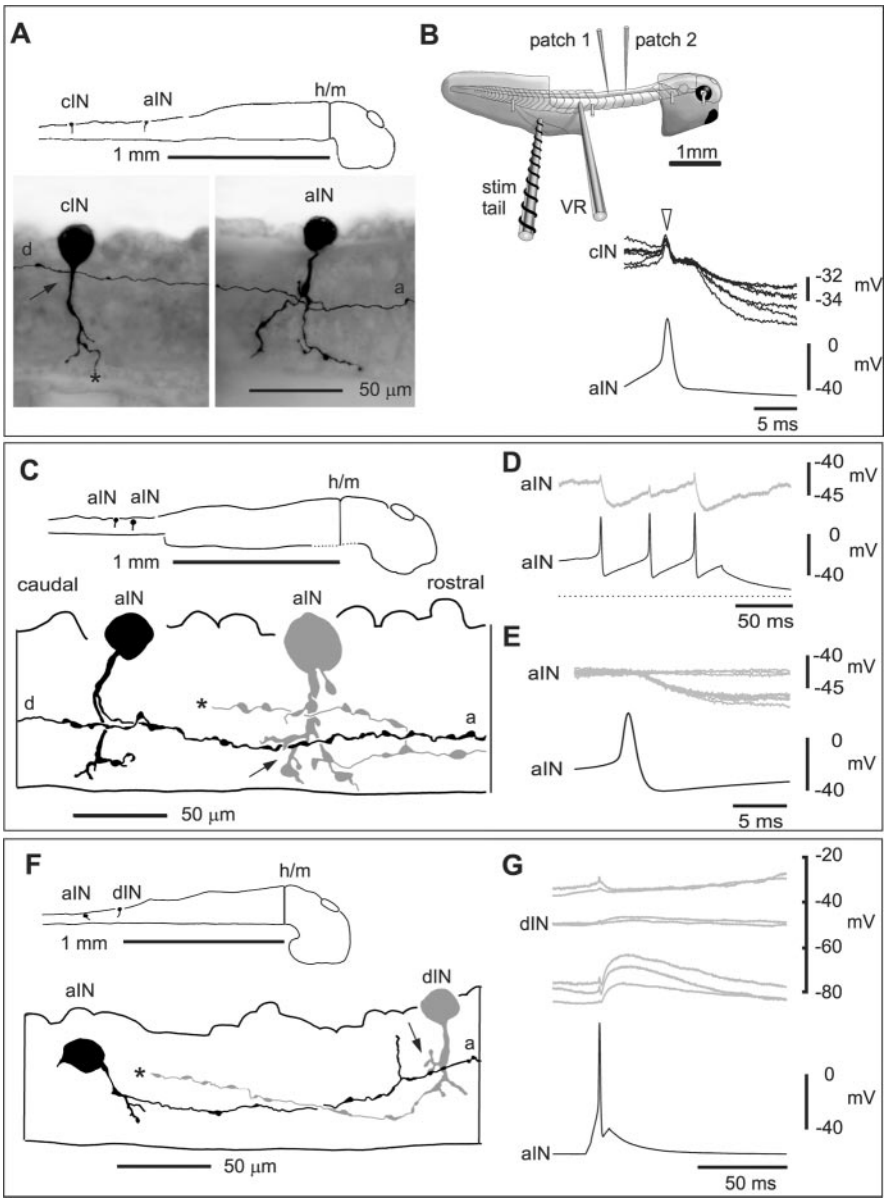

Figure 2. Diagram of the tadpole preparation and paired whole-cell recordings to show that aINs produce direct inhibition of spinal CPG neurons. *A*, Scale diagram of the CNS viewed from the right showing the location of two neurobiotin-filled neurons with a synaptic connection, shown in more detail in the micrographs below. Each neuron has a spherical soma and a ventral process with dendrites. The aIN has an ascending axon (a) and a descending axon (d) with possible synaptic contact onto a cIN dendrite (see arrow). The ventral cIN axon goes out of focus (asterisk). *B*, inset, the dissected tadpole with its spinal cord exposed is held with four micropins. Patch electrodes record two spinal neurons. Swimming can be initiated by a current pulse to excite sensory innervation of the tail skin (stim tail) and recorded from a ventral root (VR). Current-clamp recordings show impulses evoked by current injection into the aIN in *A* lead to constant latency, variable amplitude IPSPs in the cIN that was deploarized to increase IPSP amplitude (7 traces overlapped). The aIN impulse causes a cross-talk artifact in the cIN (arrowhead). *C*, Tracings to show the anatomy of two neurobiotin-filled aINs with a possible synaptic contact (arrow) from the axon of the presynaptic aIN (black) onto the postsynaptic aIN (gray), the descending axon of which is not shown beyond the asterisk. *D*, Three current-evoked impulses in the caudal aIN in *C* (dots mark its resting potential) lead to short latency IPSPs in the other aIN. The postsynaptic aIN was deploarized to increase IPSP amplitude. *E*, The same neurons as in *C*, where superimposed records show small constant latency IPSPs, with some failures, in the rostral aIN after impulses in the caudal aIN. *F*, Tracings to show the anatomy of an aIN (black) and a dIN (gray) with possible synaptic contact (arrow). The dIN descending axon is not shown further than the asterisk. *G*, Current-evoked impulses in the aIN in *F* lead to IPSPs in the dIN that can be reversed at near −40 mV by current injection into the dIN. a, Ascending aIN axon; d, descending aIN axon; h/m, hindbrain/midbrain border.

Early-cycle inhibition of CPG neurons matches aIN firing during swimming

The paired recordings establish that aINs can make direct synapses onto other spinal CPG neurons to produce glycinergic inhibition during swimming, shortly after the time at the start of each swimming cycle when most other CPG neurons fire an impulse. If aINs produce early-cycle inhibition, then their spike-firing pattern should correlate with the pattern of early-cycle IP-

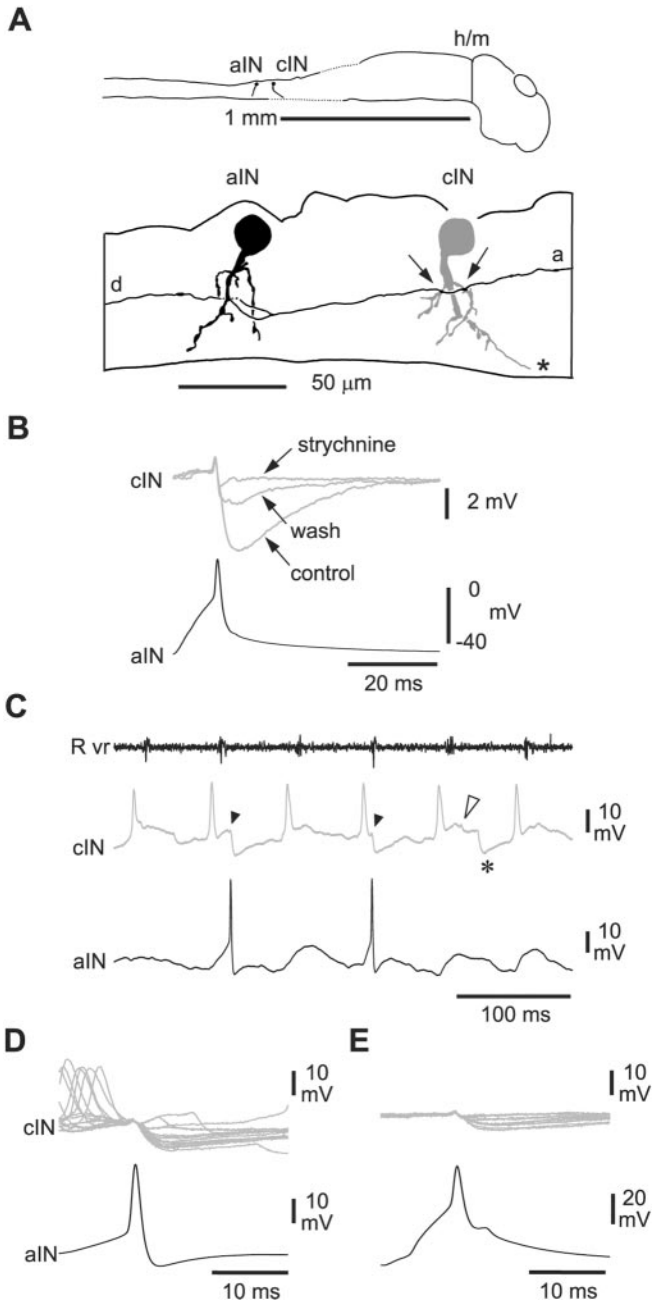

Figure 3. Inhibition from aINs is glycinergic and can produce IPSPs in CPG neurons during swimming. Recordings from an aIN and a cIN. *A*, Tracings to show the anatomy of an aIN (black) and a cIN (gray) with possible synaptic contacts (arrows) from the ascending (a) axon of the aIN. The aIN also has a descending axon branch (d). The cIN axon is not shown beyond the asterisk, where it crosses the cord ventrally. *B*, Impulses evoked in the aIN by current injection produce IPSPs in the cIN that are blocked by 5 μM strychnine, with partial recovery on wash. Each trace is the average of seven traces. *C*, Six cycles of swimming initiated by a current pulse to the skin and monitored from a ventral root on the right side (Rvr). The cIN fires a single impulse and receives IPSPs on most swimming cycles, revealed by injection of depolarizing current (asterisk, mid-cycle IPSP). The aIN fires less reliably. Two early-cycle IPSPs (arrowheads) in the cIN follow spikes in the aIN; another early-cycle IPSP does not (open arrowhead). *D*, Synchronizing records to the aIN spikes shows short latency IPSPs in the cIN follow most aIN spikes. Note that these IPSPs and the aIN spikes are not similarly time-locked to the preceding cIN spikes. *E*, IPSPs in the cIN follow spikes evoked in the aIN by current injection at the same latency as those during swimming in *D*. The IPSPs are smaller than in *D* because the cIN is less depolarized.

SPs. We have already defined the spike-firing pattern of aINs during swimming (Li et al., 2002). To define the timing of inhibitory inputs to CPG neurons during swimming, we made recordings from 87 identified neurons (47 cINs, 28 aINs, 5 dINs, and 7 mns). We first monitored their firing activity during swimming in current clamp and then recorded the same neurons under voltage clamp. By using positive holding potentials close to the EPSC reversal potential, inward currents attributable to rhythmic excitatory input could be made small enough that the occurrence and time of onset of early-cycle and mid-cycle IPSCs were clear (Fig. 4*A*,*B*). Early-cycle IPSCs, like those in Figure 4*A*, occurred in 81% of neurons (72 of 89 examined). In all 12 cases tested, they were blocked by strychnine (2–5 μM), and in all 4 cases tested, they were unaffected by bicuculline (10–20 μM). This confirmed that the early-cycle IPSCs were glycinergic, as expected if they were produced by aINs (Fig. 4*E*) (Li et al., 2002).

The timing of IPSCs was then measured in a sample from each class of CPG neuron (6 aINs, $n = 970$ cycles; 12 cINs, $n = 2447$ cycles; 5 dINs, $n = 950$ cycles; 5 mns, $n = 976$ cycles). Phase histograms (Fig. 4*C*) showed that the pattern of IPSCs during swimming was similar in each class of CPG neuron. There was a peak of early-cycle IPSCs in the first half of the cycle, followed by a much stronger peak of mid-cycle IPSCs. The relationship between the phase distribution of all early-cycle IPSCs and aIN spikes during swimming is shown graphically in Figure 4*D*. Early-cycle IPSCs in the four CPG neuron classes were closely correlated with each other and also with the timing of aIN spikes (668 spikes from 16 aINs in 16 animals; two-tailed Pearson correlation coefficient, 0.79–0.94; all $p < 0.002$). Their timing was also closely correlated with that of the glycinergic IPSPs previously described in dorsolateral commissural (dlc) sensory pathway interneurons (Fig. 4*D*, dotted line) and also produced by aINs (correlation coefficient, 0.83; $p = 0.001$) (dlc data from Li et al., 2002).

In contrast, the timing of early-cycle IPSCs was much less closely correlated with the timing of ipsilateral cIN spikes (correlation coefficient, 0.43–0.52; $p = 0.02$–0.06). cINs are the other major group of spinal, glycinergic neurons. They are responsible for reciprocal inhibition between the two sides (Dale, 1985) and could, in principle, represent a source of ipsilateral glycinergic inhibition. The relatively weak correlation between cIN spike and early-cycle IPSC timing supported two other strong pieces of evidence against this role. First, <1% of cINs have an ipsilateral axon (Li et al., 2002). Second, in 141 paired recordings between cIN and CPG neurons on the same side (100 cINs, 29 aINs, 3 dINs, and 1 mn; 8 unidentified), no inhibitory connection was found. The aINs therefore appear to be the primary source of early-cycle glycinergic inhibition in CPG neurons.

To remove mid-cycle inhibition coming from the opposite side, the ventral inhibitory connections between the two sides of the spinal cord were cut in three animals between the 2nd and 10th segment. Fictive swimming could still occur (Soffe, 1989). Recordings from eight rhythmic neurons showed that the peak of mid-cycle IPSCs during fictive swimming was absent and IPSCs were predominantly in the early phase of each swimming cycle with a similar distribution to that in intact animals (data not shown; in two cases, the peak of IPSCs was at a phase of 0.1 and 0.25). This evidence gives us additional confidence that early-cycle IPSCs originate in the same side of the spinal cord and that very few aIN-sourced IPSCs are hidden by the strong mid-cycle IPSC peak.

Individual aINs can inhibit both CPG and sensory interneurons

To test the proposal that single aINs can provide feedback inhibition of CPG interneurons as well as gating inhibition of sensory pathway interneurons during swimming, we made sequential paired recordings in four animals. In one case, connections were found from a single aIN with typical activity during swimming (Fig. 5). In the first recording, this aIN was shown to inhibit an unidentified CPG interneuron (latency, 1.2 msec) that was also active during swimming. In the second recording, the same aIN inhibited a dlc sensory pathway interneuron (latency, 1.4 msec) that was excited at a short latency after skin stimulation and that was inhibited during swimming. These recordings demonstrate that an individual aIN can produce both types of inhibition.

Early-cycle IPSCs occur more reliably at higher swimming frequencies

It has previously been shown that aIN spikes occur mainly near the start of swimming episodes (Li et al., 2002). We found that early-cycle IPSCs in CPG neurons were also more common at this time (Fig. 6*A*) and also when a stimulus was applied to the tail skin during swimming (Fig. 6*B*). These are both circumstances when the swimming frequency is usually high (Fig. 6*A–C*). Measurements for 10 CPG neurons (7 cINs, 1 mn, 1 dIN, and 1 aIN) showed that early-cycle IPSCs occurred on significantly more cycles at higher swimming frequencies (Fig. 6*D*) (Pearson correlation coefficient, 0.869; $p < 0.001$).

In summary, the evidence above demonstrates that aINs are the primary source of early-cycle, glycinergic IPSPs in CPG neurons. These IPSPs occur during the first part of the swimming cycle, slightly later than the time when most CPG neurons fire impulses that lead to the ventral root burst. The evidence also shows that this form of inhibition occurs particularly at higher swimming frequencies, such as at the start of a swimming episode.

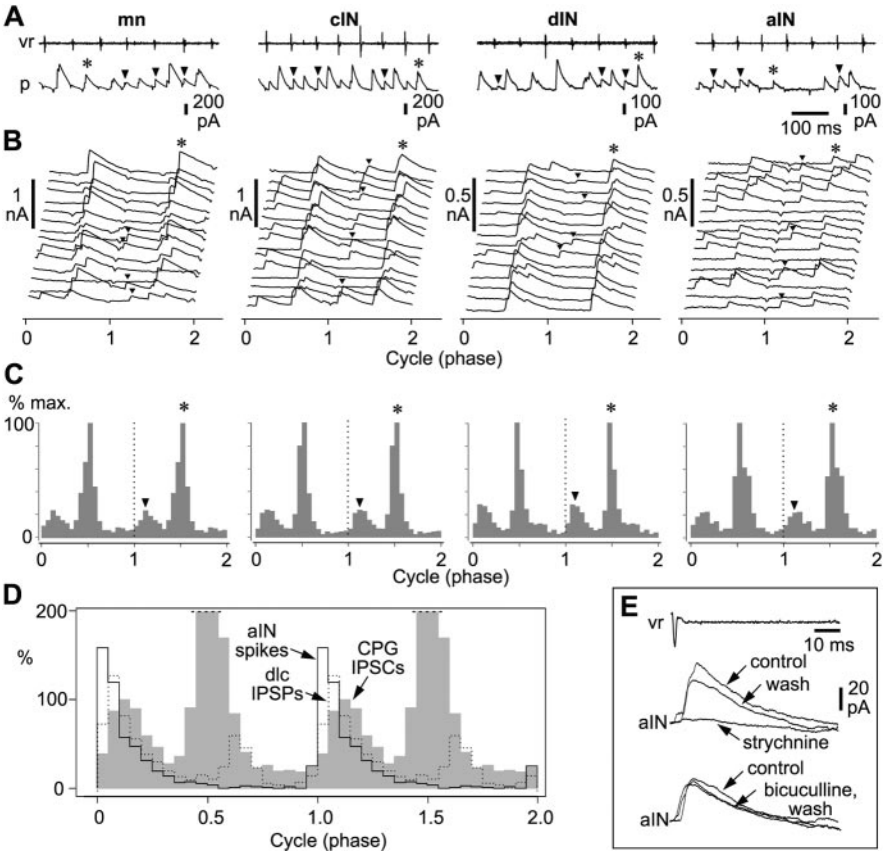

Figure 4. Pattern of early-cycle IPSCs during swimming. *A*, Voltage-clamp records made with a patch electrode (p) at positive holding potentials show IPSCs during swimming in a mn, cIN, dIN, and aIN. Swimming activity recorded from a ventral root (vr). Here, and in *B* and *C*, some early-cycle IPSCs are indicated by arrowheads and mid-cycle IPSCs by an asterisk. *B*, Waterfall plots showing the timing of IPSCs during swimming for the same recordings as in *A*. Each line shows a consecutive pair of cycles, normalized individually to a cycle phase of 1.0. Cycles are defined by the start of consecutive ventral root bursts and corrected for the longitudinal spacing between the neuron and vr recording position (which would otherwise add a timing error) (see Li et al., 2002). The second cycle on each line becomes the first cycle of the line below ($n = \sim$15 cycles per plot). *C*, Phase histograms to show the timing of IPSCs during swimming in CPG interneurons and motoneurons. Data for each cycle are plotted twice (cycle phase, 0–2), and the peak of early-cycle IPSCs is indicated (arrowhead). The numbers in each histogram bin were normalized to the mid-cycle peak value for each type of neuron (100%). In calculating correlations (see Results), the values between phase 0.35 and 0.7 were omitted to minimize the influence of mid-cycle IPSCs (asterisks), which are from cINs on the opposite side, not from aINs. *D*, The timing of early-cycle IPSCs during swimming (shaded bars are combined data from all plots in *C*) correlates well with the firing phase of aINs (solid line; total of 668 spikes in 16 aINs). The aIN spike data have been normalized to give the same total number of spikes as IPSCs between cycle phases 0 and 0.35. The dotted line shows the timing of IPSPs in sensory pathway dlc interneurons (data from Li et al., 2002). The peak in CPG IPSCs at phases of ~0.5 (mid-cycle) goes off scale. *E*, Early-cycle IPSCs in swimming, measured under voltage clamp in an aIN, are blocked by 2 μM strychnine with partial reversal but are not affected by 20 μM bicuculline. The averages are of ~15 cycles each. Traces are aligned to the onset of the cycle, indicated by the start of the ventral root burst (vr).

Early-cycle inhibition limits CPG neuron firing

Early-cycle inhibition occurs shortly after spiking of most CPG neurons. The most obvious function for such inhibition is to limit firing. Voltage-clamp recordings from CPG neurons during fictive swimming made the timing of early-cycle IPSCs clear (Fig. 7*A*). The presence of early-cycle inhibition means that the window during the first half of the swimming cycle in which firing is most likely to occur is very short (Fig. 7*A*, shaded region). Examination of swimming activity in six CPG neurons (four cINs, one aIN, and one mn) showed that there was significantly less multiple firing on cycles when early-cycle IPSPs occurred (Fig. 7*B*). In five of these neurons, positive current was injected to make the IPSPs clearer and to increase the likelihood that neurons would fire more than their usual single spike per cycle. In 218 cycles with early-cycle IPSPs, there were significantly less spikes (1.16 ± 0.37 per cycle) than in 330 cycles without early-cycle IPSPs (1.46 ± 0.55 per cycle; *F* test; $p < 0.001$). This shows that if neurons are tending to fire multiple spikes on individual swimming cycles, early-cycle inhibition can limit this firing.

En-1 labeling of spinal aINs

Evidence from the developing zebrafish shows that spinal circumferential ascending interneuron (CiA) interneurons with anatomy similar to aINs express the transcription factor En-1 (Higashijima et al., 2004). To locate the population of *En-1*-positive neurons in the *Xenopus* tadpole, we used a polyclonal antiserum, *αEnhb-1*, specific for the homeobox region of the

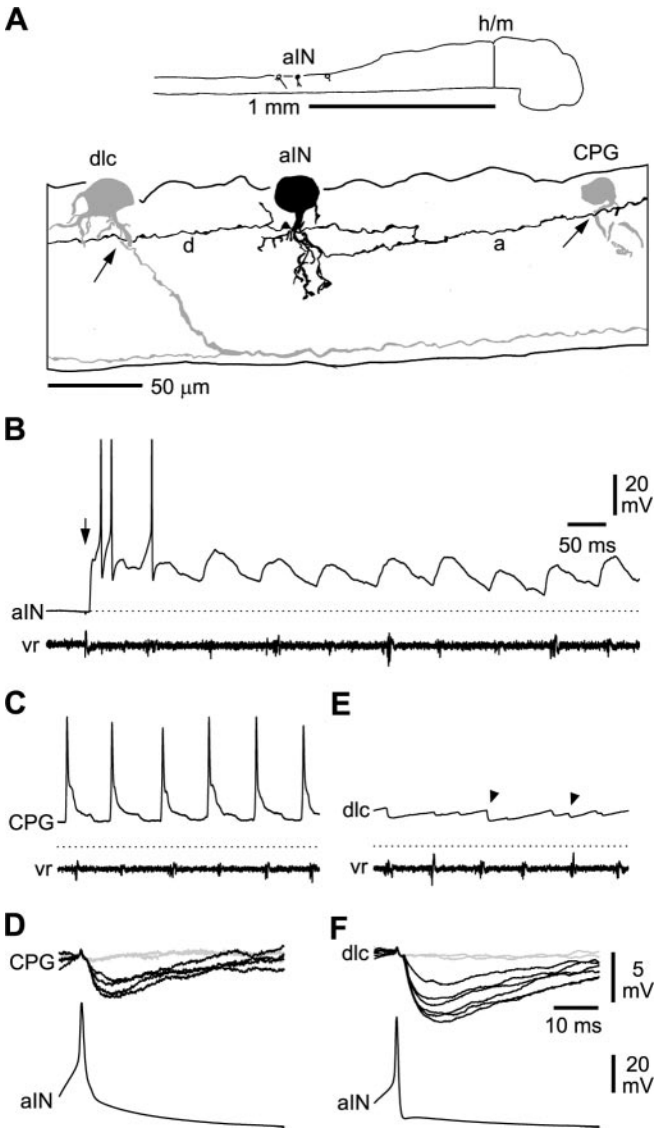

Figure 5. A single aIN inhibits both a CPG and a sensory pathway dlc interneuron. *A*, Tracings to show the anatomy of an aIN (black) and two interneurons that it contacts: an unidentified CPG interneuron (gray) with possible synaptic contacts (arrow) from the ascending axon (a) and a dlc interneuron with possible contacts (arrow) from the descending axon branch (d). The CPG neuron staining was weak, so its detailed features and axon could not be resolved. *B*, When swimming (see vr; recorded ~5 segments more caudal) is initiated by a skin stimulus (at arrow), the aIN is depolarized from the resting potential (dotted line) and fires on two cycles. *C*, During swimming, the CPG interneuron is also depolarized but fires on each cycle of swimming. *D*, In the first paired recording from this aIN, injecting current to evoke action potentials leads to variable amplitude IPSPs and some failures (gray traces) in the CPG interneuron. *E*, During swimming, the sensory pathway dlc interneuron receives some early-cycle (arrowheads) and some mid-cycle IPSPs, made larger by injection of depolarizing current. *F*, When the same aIN is recorded again with this dlc interneuron, current-evoked action potentials leads to variable amplitude IPSPs.

En-1 and En-2 proteins (Davis et al., 1991). Staining confirmed that engrailed proteins were localized in the nuclei of a longitudinal column of spinal neurons (Fig. 8*A*,*B*). At the time of hatching (stage 37/38), the total population with *En-1*-positive nuclei was 139 ± 15 neurons on each side ($n = 8$ sides). The neuron density was highest in the rostral cord and decreased caudally.

To examine whether these En-1-positive neurons had the anatomy of aINs, we labeled interneurons using either stochastic GFP labeling or retrograde filling and then stained the samples with En-1 antibody. We looked for filled neurons with En-1-positive nuclei in which we could follow the ascending axon projection and see the characteristic descending branch near the soma that is so diagnostic of aINs (Fig. 8*C*,*D*). We obtained examples in both GFP ($n = 3$) and retrograde labeling ($n = 2$) experiments. Figure 8, *C–G*, shows a GFP-labeled neuron that has the features of previously described aIN neurons and is positive for En-1. Although the evidence is still limited, it suggests that *Xenopus* aIN neurons, like the anatomically similar neurons in the zebrafish, are En-1 positive.

Discussion

The relative simplicity of the developing lower vertebrate spinal cord eases the problem of understanding spinal circuits that control simple behavior (Coghill, 1929). Recently, the whole-cell patch technique has opened up the prospect of detailed understanding in the zebrafish and frog (Saint-Amant and Drapeau, 2001; Li et al., 2002; Aiken et al., 2003). At last, spinal interneuron functions can be related to their anatomy. In the hatchling *Xenopus* tadpole, we investigated the inhibitory synaptic connections and role during swimming of aINs. This quest was made more interesting by the discovery that these neurons may, like their homologs in zebrafish embryos, express the transciption factor *En-1* (Higashijima et al., 2004) and have two distinct physiological roles. We asked first whether aINs form a single population.

Defining a primitive class of spinal inhibitory interneuron

What criteria define interneuron classes in the spinal cord? As in the rat (Silos-Santiago and Snider, 1994) and zebrafish (Bernhardt et al., 1990), the first definition of aINs in the frog tadpole was anatomical (Roberts and Clarke, 1982): unipolar soma, ventral dendrites, and characteristic axonal projection in which the ventral axon turns to ascend but branches near the soma to give a descending axon (Figs. 1, 2*C*, 3, 5) (Li et al., 2001). In these small animals, the absolute lengths of the axons of spinal neurons are usually <2 mm. Despite this, they can project over many segments (each ~0.15 mm) and for significant distances within the CNS. There is therefore no simple distinction between projection neurons and interneurons. The dorsoventral position of the aIN axons is very variable and ranges from the same dorsal level as primary sensory axons to the ventral level of motoneuron somata (Li et al., 2002).

Although we can use detailed anatomical features to define individual aINs, we cannot use them to define the whole population, so some independent, identifying characteristics are needed. In *Xenopus*, GABA-like immunoreactivity reveals a population of unipolar spinal neurons, with ascending axons, lying in a similar dorsoventral position to aINs (Roberts et al., 1987; Li et al., 2001). Fortunately, critical evidence has come from the zebrafish embryo, in which Higashijima et al. (2004) have shown that spinal CiA interneurons, with the anatomical features of *Xenopus* tadpole aINs, express the transcription factor En-1. These interneurons usually express a glycine transporter or GAD (an indicator of the presence of GABA), so are inhibitory. In *Xenopus*, our limited evidence suggests that aINs also express En-1, and a population of spinal neurons is marked by the En-1 transcription factor (Fig. 8*A*,*B*) (Davis et al., 1991). The numbers of En-1 neurons are ~20% higher than for GABA neurons for each longitudinal position, but their longitudinal distribution is very similar (Fig. 8*B*). The combination of distinctive anatomy, an inhibitory transmitter phenotype (see below), and now probable En-1 expression, gives confidence that aINs in *Xenopus* are a homogenous class of spinal interneuron.

In addition, physiological evidence provides additional consistent functional features to define this class. Whole-cell patch recordings in *Xenopus* show a characteristic firing pattern during swimming: aINs are mainly active at higher swimming frequencies and fire later and less reliably on each cycle than other CPG neurons (Figs. 3*C*, 4*D*) (Li et al., 2002). They produce glycinergic inhibition of sensory pathway and CPG neurons during swimming (Figs. 2–5), and (despite their GABA immunoreactivity) there is no evidence at this stage of development that this inhibition depends on the activation of $GABA_A$ receptors. During swimming in zebrafish, En-1-positive CiA interneurons are excited and sometimes spike in phase with nearby motor roots (Higashijima et al., 2004). Paired recording showed that CiA interneurons inhibit sensory pathway interneurons and CPG neurons.

In two developing lower vertebrates, *Xenopus* and zebrafish, there appears to be a single class of ipsilateral projecting spinal inhibitory interneuron: aINs and circumferential aINs share the same En-1 expression, glycine transmitter phenotype, detailed anatomical features (Fig. 1), and role in gating sensory pathways during swimming. This multifactor definition is a major step forward in understanding the primitive, ancestral spinal cord.

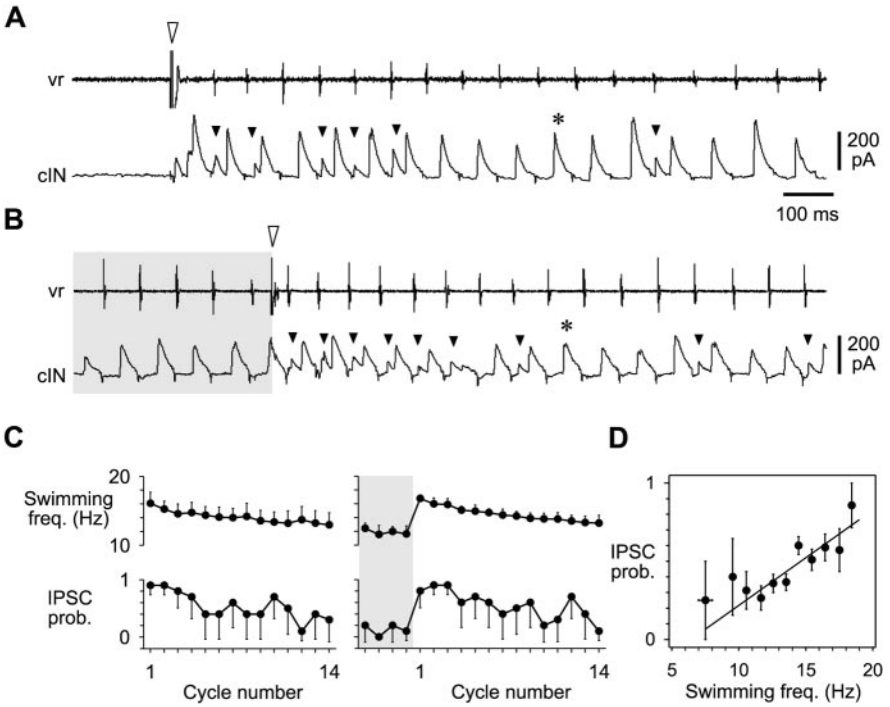

Figure 6. Early-cycle IPSCs occur more reliably at higher swimming frequencies. *A*, Recording from a ventral root (vr) and a cIN at the start of a swimming episode initiated by a skin stimulus (open arrowhead). Voltage-clamp recordings in the cIN (at a positive holding potential close to EPSC reversal level) show early-cycle IPSCs (arrowheads) when the swimming frequency is highest. These become less reliable as the swimming frequency subsequently falls (asterisk marks a mid-cycle IPSP.) *B*, Early-cycle IPSCs (arrowheads) in a cIN are more common when the swimming frequency rises after a brief tail-skin stimulus (open arrowhead) applied during swimming. They are absent immediately before the stimulus (shaded region) when the frequency is low. *C*, Swimming frequency and the probability of recording early cycle IPSCs, plotted for 10 neurons after the start of an episode of swimming (left, as in *A*) and after a stimulus applied during swimming (right, as in *B*). *D*, The probability of recording early-cycle IPSCs increases with swimming frequency. Points represent mean ± SEM for frequency and the proportion of cycles with early-cycle IPSCs for data grouped into consecutive 1 Hz bins (8–10 Hz measurements combined). The regression line was fitted to the raw data ($n = 393$ cycles; equation: $y = 0.06x - 0.40$).

Ascending interneurons have two inhibitory roles during swimming

What is the primitive function of aINs in *Xenopus*? During swimming, the spike timing of aINs correlates closely with the early-cycle inhibition of CPG interneurons and motoneurons and of sensory pathway dlc interneurons (Li et al., 2002). aIN firing and early-cycle inhibition are both most common at higher swimming frequencies. The evidence from paired recordings from aINs and sensory pathway interneurons (Li et al., 2002), and now from aINs and CPG neurons (aIN, cIN, mn, dIN), confirms that aINs provide the early-cycle inhibition in both groups of neurons. The aINs therefore appear to have two distinct roles during swimming. In CPG neurons, early-cycle inhibition provides negative feedback that can set a narrow window to help constrain firing during swimming (Fig. 7*B*). In this way, inhibition from aINs may also help to synchronize the firing of CPG neurons on the same side and lead indirectly to better alternation between the two sides. aIN inhibition may become more important later in development when *Xenopus* motoneuron fire multiply on each cycle of swimming (Sillar et al., 1991). In the case of sensory pathway dlc interneurons, aIN inhibition gates the flow of sensory input so that reflex responses are modulated to fit with ongoing swimming activity (Sillar and Roberts, 1988, 1992; Li et al., 2002). It is possible that aINs contribute to longitudinal coordination of swimming. They are also vigorously active during fictive struggling that occurs during repetitive skin stimulation (Soffe, 1993; Li et al., 2002).

aINs have long axons (length, ~1.5 mm) (Li et al., 2001), and the fills after paired recordings suggest that they make *en passant* synapses onto dendrites (Figs. 2, 3, 5). Transmission EM sections of *Xenopus* tadpole spinal cord show GABA-positive axons, very probably from aINs, making *en passant* synapses onto dendrites (Roberts et al., 1987). One aIN may therefore synapse with many neurons of different types. This makes it likely that individual aINs contact both sensory pathway and CPG interneurons. In one case, sequential paired recordings confirmed this directly (Fig. 5).

We suggest that the frog tadpole shows a primitive vertebrate condition. The spinal cord has two classes of glycinergic inhibitory interneuron that are active during swimming. One provides reciprocal inhibition (cINs) to organize the alternation of motor activity (Dale et al., 1990). The other provides recurrent inhibition (aINs) to both the sensory and motor components of the spinal circuits. Is it significant that the glycinergic sensory gating aINs may also use GABA as a transmitter? In both mouse and chick it has been proposed that embryonic spinal interneurons release GABA but later switch to glycine (Berki et al., 1995; Nakayama et al., 2002). This suggests that they have different roles at different stages of development, but there is also evidence that spinal inhibitory interneurons may co-release these transmitters simultaneously (Jonas et al., 1998). At the time of hatching, some *Xenopus* spinal interneurons in the same dorsoventral positions as aINs have both GABA and glycine immunoreactivity (A. Roberts and A. Walford, unpublished observations). Could aINs release GABA to produce presynaptic inhibition (primary afferent

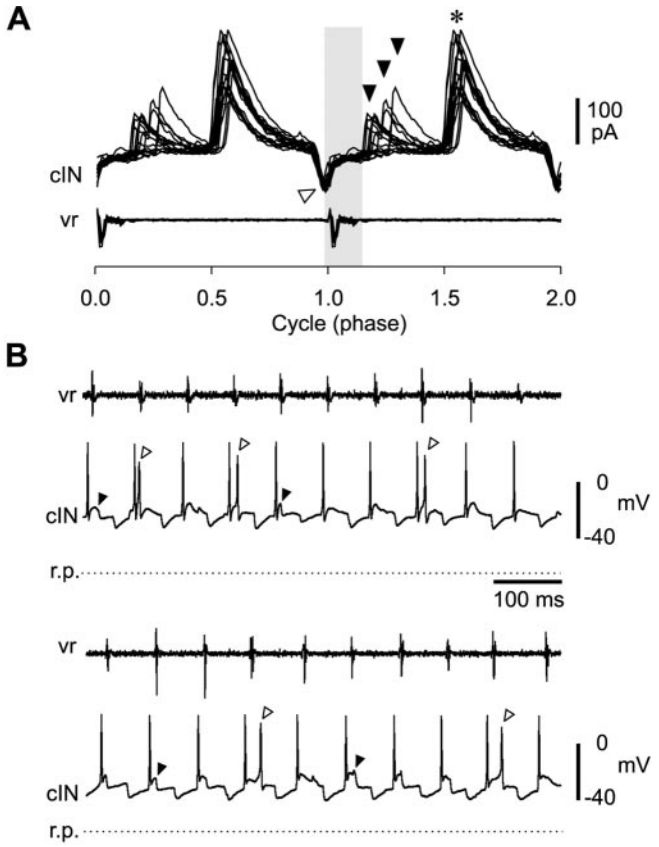

Figure 7. Early-cycle inhibition and control of multiple firing in CPG neurons. *A*, Voltage-clamp record of a cIN, clamped at a positive potential, to illustrate a typical pattern of inward (excitatory) and outward (inhibitory) PSCs during swimming. The record shows 16 overlapped cycles of swimming (mean period, 69.5 ± 2.1 msec), each normalized to a cycle phase of 1 and plotted twice. Synchronous, "on-cycle" EPSCs (open arrowhead) just precede the start of the ventral root burst (vr; timing adjusted for longitudinal spacing of electrodes). Early-cycle IPSCs from aINs (filled arrowheads) are delayed relative to the on-cycle excitation and are less synchronized than on-cycle EPSCs or mid-cycle IPSCs from contralateral cINs (asterisk). The shaded region shows the window for impulse firing before early-cycle inhibition. *B*, Examples of firing activity in two cINs during swimming shown with ventral root activity (vr). Early-cycle IPSPs are present on some cycles (e.g., arrowheads). However, the neurons fire more impulses on cycles where these are absent (open arrowheads).

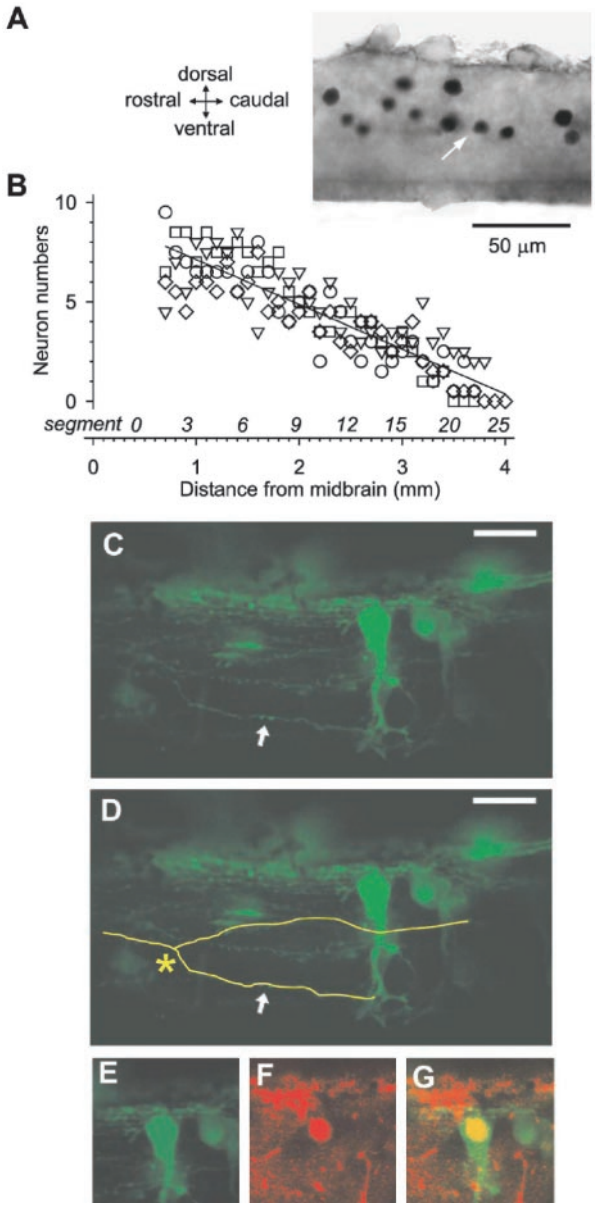

Figure 8. The distribution of En-1-positive neurons. *A*, En1-positive nuclei of neurons on one side of the whole spinal cord seen in an optical section at 1.5 mm caudal to the midbrain. Dark stained nuclei (e.g., at white arrow) form a column in a middle dorsoventral position. *B*, The distribution of spinal En1-positive neurons as a function of distance from the midbrain. The plot shows the mean number of neurons (aINs are marked nuclei) on each side for consecutive 0.1 mm blocks in four tadpoles (different symbol for each; regression line: $y = 9.37 - 2.25x$). *C*, An aIN with the ascending axon (arrow) clearly visible is labeled by GFP. The neuron is unipolar with dendrites near the point at which the main axonal process turns rostrally. Scale bar, 20 μm. *D*, aIN in *C* with ascending axon marked in yellow to show descending branch (at asterisk). *E–G*, Images of the aIN in *C* to show the En1-positive nucleus (red) lies within the aIN cell body.

depolarization) in primary afferent terminals like that found in mammals (Rudomin and Schmidt, 1999) or indeed control their own transmitter release (Lim et al., 2000)?

Do developing spinal interneurons share features across the major classes of vertebrates? Studies have now been performed on the fish, frog, chick, and mouse. In all these examples, spinal En-1 neurons lie in a mid-dorsoventral position, have an ascending, ipsilateral axon, and are thought to be inhibitory (Burrill et al., 1997; Matise and Joyner, 1997; Saueressig et al., 1999; Wenner et al., 2000; Sapir et al., 2004). It is interesting that in both the developing fish (Higashijima et al., 2004) and frog tadpole, neurons that may express En-1 provide inhibition during swimming to the motor system of the spinal CPG but also provide gating inhibition to sensory pathways during swimming. We suggest that early in development (and primitively in vertebrates) a single class of recurrent inhibitory interneurons (aINs in *Xenopus*) serves a range of different functions that later in development (and in higher groups like mammals) will be performed by separate classes of more specialized interneurons. One possibility is that later in development more dorsal aINs differentiate to become specialized for sensory pathway inhibition and more ventral ones for motor system inhibition.

References

Aiken SP, Kuenzi FM, Dale N (2003) Xenopus embryonic spinal neurons recorded in situ with patch-clamp electrodes–conditional oscillators after all? Eur J Neurosci 18:333–343.

Berki AC, O'Donovan MJ, Antal M (1995) Developmental expression of glycine immunoreactivity and its colocalization with GABA in the embryonic chick lumbosacral spinal cord. J Comp Neurol 362:583–596.

Bernhardt RR, Chitnis AB, Lindamer L, Kuwada JY (1990) Identification of

spinal neurons in the embryonic and larval zebrafish. J Comp Neurol 302:603–616.
Buchanan JT (2001) Contributions of identifiable neurons and neuron classes to lamprey vertebrate neurobiology. Prog Neurobiol 63:441–466.
Burrill JD, Moran L, Goulding MD, Saueressig H (1997) PAX2 is expressed in multiple spinal cord interneurons, including a population of EN1+ interneurons that require PAX6 for their development. Development 124:4493–4503.
Coen L, du Pascier D, Le Mevel S, Brown S, Tata J, Marabrand A, Demeneix BA (2001) Xenopus Bcl-X(L) selectively protects Rohon-Beard neurons from metamorphic degeneration. Proc Natl Acad Sci USA 98:7869–7874.
Coghill GE (1929) Anatomy and the problem of behaviour. London: Cambridge UP.
Dale N (1985) Reciprocal inhibitory interneurones in the Xenopus embryo spinal cord. J Physiol (Lond) 363:61–70.
Dale N, Roberts A, Soffe SR (1990) The anatomy, development, physiology and role of glycinergic neurons in the Xenopus embryo spinal cord. In: Glycine neurotransmission (Ottersen OP, Storm-Mathisen J, eds), pp 329–353. Chichester, UK: Wiley.
Davis CA, Holmyard DP, Millen KJ, Joyner AL (1991) Examining pattern formation in mouse, chicken and frog embryos with an En-specific antiserum. Development 111:287–298.
Goulding M, Lanuza G, Sapir T, Narayan S (2002) The formation of sensorimotor circuits. Curr Opin Neurobiol 12:508–515.
Hale ME, Ritter DA, Fetcho JR (2001) A confocal study of spinal interneurons in living larval zebrafish. J Comp Neurol 437:1–16.
Helms AW, Johnson JE (2003) Specification of dorsal spinal cord interneurons. Curr Opin Neurobiol 13:42–49.
Higashijima S, Masino MA, Mandel G, Fetcho JR (2004) Engrailed-1 expression marks a primitive class of inhibitory spinal interneuron. J Neurosci 24:5827–5839.
Jankowska E (2001) Spinal interneuronal systems: identification, multifunctional character and reconfigurations in mammals. J Physiol (Lond) 533:31–40.
Jonas P, Bischofberger J, Sandkuhler J (1998) Corelease of two fast neurotransmitters at a central synapse. Science 281:419–424.
Lee SK, Pfaff SL (2001) Transcriptional networks regulating neuronal identity in the developing spinal cord. Nat Neurosci [Suppl] 4:1183–1191.
Li WC, Perrins R, Soffe SR, Yoshida M, Walford A, Roberts A (2001) Defining classes of spinal interneuron and their axonal projections in hatchling Xenopus laevis tadpoles. J Comp Neurol 441:248–265.
Li WC, Soffe SR, Roberts A (2002) Spinal inhibitory neurons that modulate cutaneous sensory pathways during locomotion in a simple vertebrate. J Neurosci 22:10924–10934.
Li WC, Soffe SR, Roberts A (2003) The spinal interneurons and properties of glutamatergic synapses in a primitive vertebrate cutaneous flexion reflex. J Neurosci 23:9068–9077.
Lim R, Alvarez FJ, Walmsley B (2000) GABA mediates presynaptic inhibition at glycinergic synapses in a rat auditory brainstem nucleus. J Physiol (Lond) 525:447–459.
Matise MP, Joyner AL (1997) Expression patterns of developmental control genes in normal and Engrailed-1 mutant mouse spinal cord reveal early diversity in developing interneurons. J Neurosci 17:7805–7816.
Nakayama K, Nishimaru H, Kudo N (2002) Basis of changes in left-right coordination of rhythmic motor activity during development in the rat spinal cord. J Neurosci 22:10388–10398.
Parker D (2003) Activity-dependent feedforward inhibition modulates synaptic transmission in a spinal locomotor network. J Neurosci 23:11085–11093.
Parker D, Grillner S (2000) The activity-dependent plasticity of segmental and intersegmental synaptic connections in the lamprey spinal cord. Eur J Neurosci 12:2135–2146.
Roberts A (1990) How does a nervous system produce behaviour? A case study in neurobiology. Sci Prog 74:31–51.
Roberts A (2000) Early functional organization of spinal neurons in developing lower vertebrates. Brain Res Bull 53:585–593.
Roberts A, Clarke JDW (1982) The neuroanatomy of an amphibian embryo spinal cord. Philos Trans R Soc Lond B Biol Sci 296:195–212.
Roberts A, Dale N, Ottersen OP, Storm-Mathisen J (1987) The early development of neurons with GABA immunoreactivity in the CNS of Xenopus laevis embryos. J Comp Neurol 261:435–449.
Rudomin P, Schmidt RF (1999) Presynaptic inhibition in the vertebrate spinal cord revisited. Exp Brain Res 129:1–37.
Saint-Amant L, Drapeau P (2001) Synchronization of an embryonic network of identified spinal interneurons solely by electrical coupling. Neuron 31:1035–1046.
Sapir T, Geiman EJ, Wang Z, Velasquez T, Mitsui S, Yoshihara Y, Frank E, Alvarez FJ, Goulding M (2004) Pax6 and engrailed 1 regulate two distinct aspects of renshaw cell development. J Neurosci 24:1255–1264.
Saueressig H, Burrill J, Goulding M (1999) Engrailed-1 and netrin-1 regulate axon pathfinding by association interneurons that project to motor neurons. Development 126:4201–4212.
Sillar KT, Roberts A (1988) A neuronal mechanism for sensory gating during locomotion in a vertebrate. Nature 331:262–265.
Sillar KT, Roberts A (1992) Phase-dependent modulation of a cutaneous sensory pathway by glycinergic inhibition from the locomotor rhythm generator in Xenopus embryos. Eur J Neurosci 4:1022–1034.
Sillar KT, Wedderburn JF, Simmers AJ (1991) The development of swimming rhythmicity in post-embryonic Xenopus laevis. Proc R Soc Lond B Biol Sci 246:147–153.
Silos-Santiago I, Snider WD (1994) Development of interneurons with ipsilateral projections in embryonic rat spinal cord. J Comp Neurol 342:221–231.
Soffe SR (1989) Roles of glycinergic inhibition and N-methyl-D-aspartate receptor mediated excitation in the locomotor rhythmicity of one half of the Xenopus embryo central nervous system. Eur J Neurosci 1:561–571.
Soffe SR (1993) Two distinct rhythmic motor patterns are driven by common premotor and motor neurons in a simple vertebrate spinal cord. J Neurosci 13:4456–4469.
Tunstall MJ, Roberts A (1994) A longitudinal gradient of synaptic drive in the spinal cord of Xenopus embryos and its role in co-ordination of swimming. J Physiol (Lond) 474:393–405.
Wenner P, O'Donovan MJ, Matise MP (2000) Topographical and physiological characterization of interneurons that express engrailed-1 in the embryonic chick spinal cord. J Neurophysiol 84:2651–2657.